PROPULSIVE PERFORMANCE OF THE AUTONOMOUS UNDERWATER VEHICLE "C-SCOUT"

Roy Thomas[1], Neil Bose[2] and Christopher D. Williams[3]

[1]M.Eng. Student, [2]Canada Research Chair in Offshore and Underwater Vehicles Design
Ocean and Naval Architectural Engineering
Memorial University of Newfoundland
St. John's, NL, Canada, A1B 3X5
http://www.engr.mun.ca
Email: Roy.Thomas@nrc-cnrc.gc.ca, nbose@engr.mun.ca

[3]Research Engineer (Underwater Vehicles)
National Research Council Canada, Institute for Marine Dynamics
Box 12093, Postal Station 'A', St. John's, NL, Canada, A1B 3T5
http://imd-idm.nrc-cnrc.gc.ca/, www.c-scout.net
Email: Christopher.Williams@nrc-cnrc.gc.ca

Abstract

The autonomous underwater vehicle "C-SCOUT" is being jointly developed by the National Research Council Canada - Institute for Marine Dynamics (NRC-IMD) and the Ocean Engineering Research Centre at Memorial University of Newfoundland (MUN-OERC) with the support of several Canadian companies and universities. In its current configuration, the vehicle is torpedo-shaped, with an overall length of 2.70 metres and a diameter of 0.40 metres. In December 2002, the authors conducted propulsion tests on the full scale "C-SCOUT" vehicle, at the towing tank of the OERC. This paper reports results from those tests.

Introduction

As ocean exploration heads into deeper waters, autonomous underwater vehicles (AUVs) are increasingly emerging as a commercially viable technology. The AUV "C-SCOUT" is being developed as part of a larger NSERC Strategic Project titled "Offshore Environmental Risk Engineering using Autonomous Underwater Vehicles". This project is concerned with the development of AUVs for environmental monitoring missions, in order to assess the impact of discharges from offshore oil and gas operations.

All AUV designers strive to improve the endurance of their AUVs. Endurance refers to the range (distance) or time that an AUV can travel at sea, while working on a mission, given a fixed amount of energy which is stored on board the vehicle. Endurance is a measure of the overall efficiency of an AUV.

Two components that contribute to this overall efficiency are resistance and propulsion. The lower the vehicle resistance, the higher its endurance. Similarly, the higher the efficiency of the propulsion system, the higher is the vehicle endurance.

In order to improve the efficiency of the propulsion system and reduce the drag of the vehicle, one must first be able to quantify what their values are, hence resistance and self-propulsion tests are one step in gaining this information. Resistance, self-propulsion and bollard-pull tests were conducted, on a full scale version of the "C-SCOUT" vehicle, in a towing tank (54.7 x 4.57 x 2.5 m).

The "C-SCOUT" Vehicle

The current version of the vehicle (known as the "baseline version") has been designed to be streamlined in shape, with an ellipsoidal nose, cylindrical mid-body, and a cubic-spline tail [Figure 1]. The AUV has been designed and constructed using modular sections, so that it can be easily adapted to a wide variety of configurations, depending on its mission. These modules include the nose module, the forward and aft battery modules, the pressure vessel module, the aft fin module and the tail module.

The vehicle is propelled using a 0.75kW (one HP) ducted thruster and is powered using six lead-acid gel batteries. Four fins (NACA-0012 sections) have been provided for maneuvering the vehicle in the horizontal and vertical planes. The vehicle electronics are housed in a sealed pressure vessel and the electronics are based on a Distributed Embedded Modular Architecture (DEMA) [Reference 1].

1.0 Resistance and Self-Propulsion Tests

1.1 Test Setup

A bare-hull version of the "C-SCOUT" vehicle (2.70 m long, 0.40 m diameter) was outfitted with a propulsion system for these tests. The vehicle was immersed 0.9 m below the water surface [Figure 2, Figure 3]. Two faired vertical struts, one at each end of the vehicle, were used to support the vehicle in the water. The top ends of these struts were attached to a support frame, which was attached to the towing carriage. The bottom ends of the struts were attached to the vehicle forward and aft through flexible supports. Each of these flexible supports had three leaf springs mounted in a Y-shaped configuration [Figure 4, Figure 5]. The outer end of each leaf spring was attached to the vehicle hull while the inner end of each leaf spring was attached to its strut. These leaf springs constrained the vehicle to move only forward and aft, relative to the struts.

The forward flexible support housed a single-axis load cell (450 N capacity). This load cell was attached between the forward strut and the hull, in order to measure the force required to tow the vehicle through the water. Inside the vehicle, in the free space between the forward and aft flexible supports, a pressure vessel was fitted. This pressure vessel housed the main propulsion motor (Aerotech model 1960 DC motor) and a thrust and torque dynamometer (Kempf and Remmers model 25). The propulsion motor had an built-in tachometer for measuring the rotational speed of the propeller shaft. This motor was used for the self-propulsion tests and is not the motor used on the regular vehicle for propulsion.

The pressure vessel was charged with nitrogen gas (15 kPa), so as to keep the internal pressure of the cylinder slightly higher than the outside water pressure and thereby preclude the possibility of water ingress into the pressure vessel, in case of leakage at the stern tube seal. Nitrogen gas was supplied to the pressure vessel using a portable nitrogen bottle placed on the towing carriage; a flexible hose supplied gas from the bottle to the pressure vessel.

The stern tube housed the propulsion shafting. The propeller shaft consisted of a hardened steel shaft which was coupled to the thrust and torque dynamometer at the inboard end and had the propeller mounted on its outboard end. The shaft was supported by three linear rotary bearings, fitted at equal distances apart, inside the stern tube. The linear rotary bearings permitted the shaft to rotate, as well as to slide freely in the axial direction. This ensured that all thrust developed by the propeller was transmitted directly to the dynamometer and that there was no loss of measured thrust due to over-tight bearings.

At the location where the propeller shaft penetrated the cover plate of the pressure vessel, two lip seals (fitted back to back) were used for sealing purposes. The propeller, hub and accelerating duct used for these tests were identical to that of the commercially available Tecnadyne model 1020 thruster.

An Omega OM3 series signal conditioner was used for amplifying and filtering the analogue output signals from the different transducers (load cell, dynamometer, tachometer). A DaqBoard 2000 data acquisition card, fitted into the PCI slot of a Pentium desktop computer, was used as the data acquisition system. This card was controlled and operated by the DaqView data acquisition software. The DaqBoard 2000 card had a built-in 16 bit, 200 kHz analog to digital converter, which converted the continuous analogue signals from the signal conditioner into digital signals. The acquired data were processed and stored on the hard drive of the computer in ASCII format.

1.2 Test Procedure

The load cell and the dynamometer were mechanically calibrated by subjecting them to known loads and torques and then noting the output voltages of these transducers. The propulsion motor tachometer was calibrated by running the motor at a number of speeds and recording the output voltage of the tachometer; the motor speed was measured using a portable optical tachometer.

Subsequently the in-situ tests and checks were performed. These included an alignment check of the vehicle and leaf springs (Figure 6), an axial pull check and shaft friction torque tests. Thereafter the in-water tests commenced.

The test program included the following tests: (i) resistance tests, (ii) bollard-pull tests, and, (iii) load-varying self-propulsion tests [Reference 2]. For the resistance tests, the vehicle was towed at a series of constant speeds, in both the forward and reverse directions. First the bare hull was towed, in order to measure the resistance due to the bare hull alone. Next the propeller was fitted, in order to measure the additional resistance due to the (free-wheeling) propeller. Finally the duct was fitted, in order to measure the additional resistance due to the duct. For the bollard-pull tests with the towing carriage stationary, the propulsive thrust and torque were measured, with and without the duct. For the self-propulsion tests, the vehicle was towed at a combination of towing speeds and propeller shaft speeds, in the forward direction; here the towing force and propulsive thrust and torque were measured, with and without the duct. By performing these different types of tests, one can isolate the effects of the hull, propeller and duct and thus obtain a measure of the overall system efficiency, as well as an insight into where further improvements in efficiency can be obtained. Details of the tests and analysis methods have been published by Thomas [Reference 3].

1.3 Test Results

1.3.1 Load-Varying Self-Propulsion Tests

One of the primary objectives of these tests was to evaluate the propulsive performance of the vehicle, using load-varying self-propulsion tests. The load-varying self-propulsion tests included two phases. Phase I tests were performed with only the propeller fitted onto the vehicle. Phase II tests were performed with both the propeller and duct fitted onto the vehicle. Each of the two sets of tests were conducted using the following speeds of the towing carriage: 0.8, 1.1, 1.3, 1.6, 1.8, 2.1, 2.3 and 2.5 m/s. At each towing speed, the propeller shaft speed was systematically varied so as to cover the entire range of propeller loadings. Each test used the following shaft speeds: 500, 550, 600, 650, 750, 900, 1000, 1050, 1100, 1150, 1200 and 1250 RPM. At shaft speeds below 500 RPM, the thrusts and torques generated by the propeller were too small in magnitude to be measured accurately, hence no tests were conducted below 500 RPM.

The results from Phases I and II were then utilized to determine the duct thrust, using the procedure described in section 1.3.2. The duct thrust was then added to the propeller thrust in order to obtain the total thrust of the propulsor.

For the Phase I tests, the tow force (ordinate) was plotted against the propeller thrust (abscissa). For the Phase II tests, the tow force (ordinate) was plotted against the total propulsor thrust (abscissa) as shown in Figure 7.

Both plots were found to be linear and hence they satisfied the linearity axiom for load-varying self-propulsion tests [Reference 4, 5, 6]. Using regression analysis, straight lines were fitted through the data points. Each straight line represents a particular vehicle speed (V) at which the self-propulsion test was conducted. The equation of each straight line is of the form

$$F = -(1 - t^*)\cdot T + F_{T=0}$$

where 'F' is the measured tow force, 'T' is the measured propulsor thrust, and '$F_{T=0}$' is the value of the tow force when the propulsor thrust is zero, that is, the intercept on the ordinate axis of Figure 7. From these equations, the vehicle resistance under idling propeller conditions, $F_{T=0}$, and the thrust deduction fraction (t*) were determined; see Table 1. Since the full scale "C-SCOUT" vehicle was used for these tests, therefore the self-propulsion point of the vehicle is that point when the tow force (F) becomes equal to zero. Substituting F = 0 in the above equation, the values of the propulsor thrust, at each self-propulsion point (T_s), were determined; see Table 1.

The measured values of the vehicle speed, propeller rotational speed, propeller torque, propeller thrust and tow force were then used to form non-dimensional thrust, torque, tow force and advance coefficients, according to the following definitions. For the Phase I tests, these coefficients are the propeller thrust coefficient 'K_{tp}', propeller torque coefficient 'K_q', tow force coefficient 'K_{fd}' and advance coefficient 'J'. For the Phase II tests, these coefficients are the propeller thrust coefficient 'K_{tp}', duct thrust coefficient 'K_{td}', total thrust coefficient 'K_{tt}', propeller torque coefficient 'K_q', tow force coefficient 'K_{fd}' and advance coefficient 'J'. Here 'ρ' is the mass density of water, 'n' is the propeller rotational speed, 'D' is the propeller diameter and 'V' is the vehicle (towed) speed.

$K_{td} = T_d / \{\rho\cdot n^2\cdot D^4\}$ - thrust coefficient for the duct
$K_{tp} = T_p / \{\rho\cdot n^2\cdot D^4\}$ - thrust coefficient for the propeller
$K_{tt} = K_{tp} + K_{td}$ - thrust coefficient for the propeller + duct
$K_q = Q / \{\rho\cdot n^2\cdot D^5\}$ - torque coefficient for the propeller
$K_{fd} = F / \{\rho\cdot n^2\cdot D^4\}$ - tow force coefficient
$J = V / \{n\cdot D\}$ - advance ratio for the propeller

For the Phase I tests, these coefficients were plotted as curves of K_{tp} vs J, $10K_q$ vs J and K_{fd} vs J, as shown in Figure 8. For the Phase II tests, these coefficients were plotted as curves of K_{tp} vs J, K_{td} vs J, K_{tt} vs J, $10K_q$ vs J and K_{fd} vs J, as shown in Figure 9.

The self-propulsion point in these plots can also be determined by inserting an additional curve of thrust coefficient 'K_{ts}' as a function of J^2 into the plots. The coefficient 'K_{ts}' is defined as

$$K_{ts} = T_s\cdot J^2 / \{\rho\cdot D^2\cdot V^2\}$$

where 'T_s' is the propulsor thrust at self-propulsion point. For the Phase I tests, the intersection of the 'K_{ts}' curve and the 'K_{tp}' curve represents the self-propulsion point of the vehicle; an example is shown in Figure 8, for a vehicle speed of 1.3 m/s. For the Phase II tests, the intersection of the 'K_{ts}' curve and the 'K_{tt}' curve represents the self-propulsion point of the vehicle, see Figure 9, again for a vehicle speed of 1.3 m/s. Note that in each Figure, the curve of 'K_{fd}' crosses the J-axis, indicating that the tow force is zero at the self-propulsion point.

From the self-propulsion point, the propeller torque coefficient '$10K_q$' and the advance coefficient 'J' were read off. These were then used to determine the propeller rotational speed 'n' and the delivered power 'P_d' at the self-propulsion point, using the following expressions.

$$n = V / \{J\cdot D\}$$

and

$$P_d = 2\pi\rho n^3 D^5 K_q$$

The effective power 'P_e' of the vehicle was then calculated from

$$P_e = V\cdot F_{T=0}$$

Subsequently the propulsive efficiency 'η_d' of the propulsion system was calculated from

$$\eta_d = P_e / P_d$$

The results for the Phase II tests are tabulated in Table 1. Figure 10 shows a plot of delivered power and effective power vs forward speed. Figure 11 shows a plot of propulsive efficiency vs forward speed.

1.3.2 Duct Thrust Measurement Method

The test setup for the self-propulsion tests was used for the duct thrust measurements. In this case direct measurement of duct thrust is required, so the duct needs to be supported by its own load cell, which is in turn supported by a rigid structure. In a conventional test where the vehicle is attached rigidly to the struts, this load cell would be attached to the aft strut or to the support frame.

But for these tests, since the vehicle was not attached rigidly to the struts, the load cell for measuring duct thrust could no longer be attached to the aft strut or to the support frame, but instead would have had to be directly attached to the vehicle hull. Such an arrangement invariably causes the flow pattern around the aft end of the vehicle to get altered, thereby changing the test results. Further, the entire arrangement for supporting the vehicle using flexible supports was already quite complicated and fitting an additional load cell and its support structure was not found to be practical. Therefore it was decided not to measure the duct thrust directly, but instead to infer the duct thrust from the results from the tests of Phases I and II.

Figure 12 shows the forces acting on the vehicle during the course of Phases I and II. $F_{T=0}$ is essentially the same in both the cases. If the augment in resistance (a thrust-deduction effect of propulsor) is assumed to be same in both the cases, then the duct thrust can be inferred using the following expression:

Duct Thrust = [Tow Force(II) – Propeller Thrust(II)] - [Tow Force(I) – Propeller Thrust(I)]

Using the above expression, the duct thrust was inferred at each propeller speed for which a self-propulsion test was conducted. This duct thrust was then added to the propeller thrust, in order to obtain the total thrust generated by the propulsor, at each propeller speed for which a self-propulsion test was conducted.

1.3.3 Bollard Pull Tests

The bollard pull of a vehicle is essentially a measure of the greatest towing force the vehicle can exert on a towline, while the vehicle is stationary (zero forward speed). The vehicle was fitted with both the propeller and the duct for these tests. Bollard pull tests were conducted by keeping the vehicle stationary and then systematically varying the propeller speed. At each propeller speed, the following parameters were recorded: propeller speed, propeller thrust, shaft torque, tow force and water temperature. The recorded data were then used to make plots of tow force versus propeller speed (Figure 13), and of delivered power versus propeller speed (Figure 14).

1.3.4 Bare Hull Resistance Tests

Resistance tests were conducted in order to determine the drag (resistance) of the bare hull of the vehicle. The propeller and duct were removed for these tests. The vehicle was towed over a range of speeds in the ahead as well as astern directions. The parameters recorded included the carriage speed, vehicle resistance and the water temperature. Tests were not conducted at speeds below 0.6 m/s, since the measured resistance at speeds below 0.6 m/s was too small to be reliably measured by the load cell. For the astern direction, the tests were limited to a maximum speed of 2 m/s, since the towing carriage could go no faster than 2 m/s when traveling backwards.

The measured data were then used to create plots of vehicle resistance versus vehicle speed, for both the ahead and astern conditions, Figures 15 and 16. The data were also non-dimensionalized into a drag coefficient 'C_d'; the frontal area $\pi D^2/4$ of the vehicle was used for calculating the drag coefficient. The drag coefficient 'C_d' was then plotted against the vehicle forward speed; see Figure 17. At speeds above 2 m/s, the rise of 'C_d' indicates a higher than V^2 dependence of resistance on speed (V).

Since the depth of the towing tank was limited, therefore the vehicle could only be submerged to a centreline depth of 0.91 m, 2.2 body diameters) below the free surface of water. As a rule of thumb, the body needs to be submerged at least five body diameters below the surface of water, in order to completely preclude free surface (wave making) effects [Reference 7]. Consequently at towing speeds above 2 m/s, a significant amount of wave making resistance showed up in the data. This is indicated by a sharp jump in the vehicle resistance above 2 m/s, Figure 15. Below towing speeds of 2 m/s, the vehicle resistance is predominantly viscous and there is a uniform parabolic-type increase in resistance with increasing forward speeds.

The vehicle resistances in the ahead and astern directions were compared, Figure 16. The resistance values (towing forces) were close to each other at lower speeds. With increasing speeds, the difference in resistance increased and then stabilized to a more or less constant difference of about 12 percent. The vehicle resistance in the ahead direction (R) was also compared with the magnitude of the tow force when the propulsor thrust was zero ($F_{T=0}$); Figure 18. The values of R and $F_{T=0}$ were close to each other at lower speeds. At higher speeds the difference in R and $F_{T=0}$ stabilized to a more or less constant value of about 9.8 percent.

Conclusion

These resistance and propulsion experiments with "C-SCOUT", constitute a first step in evaluating the vehicle performance. They provide a wealth of information about the performance of the propulsion system over a range of vehicle speeds and propeller loadings. This data will be used for optimizing the propulsion system and the hull form of the vehicle. Work is ongoing on the design of a slow-speed high-efficiency propeller and on the design of a cyclic-pitch-propeller propulsion and control system.

Acknowledgements

We thank the Natural Sciences and Engineering Research Council (NSERC), Canada, for financial support through the Strategic Project “Offshore environmental engineering using autonomous underwater vehicles”. We also thank the National Research Council Canada – Institute for Marine Dynamics, St John’s, for providing equipment and technical support for these tests.

References

1. Taylor, S., Simms, M., O'Young, S. and Bose, N., "Distributed Embedded Modular Architecture (DEMA) for Autonomous Underwater Vehicle (AUV) Control Systems". Proceedings UUST'03, Durham, New Hampshire, August 2003.

2. Murdey, D.C., NRC Institute for Marine Dynamics Standard Test Methods: "Resistance in Open Water", 42-

8595-S/TM-1, version 5, 09 March 2001; "Propeller Open Water Tests", 42-8595-S/TM-2, version 4, 20 February 2002; "Model Propulsion in Open Water", 42-8595-S/TM-3, version 4, 06 March 2002; St. John's, Newfoundland, Canada.

3. Thomas, R., "Performance Evaluation of the Propulsion System of the Autonomous Underwater Vehicle "C-SCOUT". Master's Degree Thesis, 2003, Faculty of Engineering and Applied Science, Memorial University of Newfoundland, Canada.

4. Kracht, A.M, "Load Variation Tests Improve the Reliability of Ship Power Predictions Based on Model Test Results", Schiffstechnik 38, 1991, Germany.

5. Holtrop, J., "Extrapolation of Propulsion Tests for Ships with Appendages and Complex Propulsors", Marine Technology, SNAME, Vol. 38, No. 3, July 2001, USA.

6. Molloy, S., "Ship Powering Prediction Using Load Varying Self-Propulsion Tests", Master's Degree Thesis, 2001, Faculty of Engineering and Applied Science, Memorial University of Newfoundland, Canada.

7. Hoerner, S.F., "Fluid Dynamic Drag", Published by the Author, 1965.

Table 1 **(Phase II)**

Self-Propelled Condition, Ahead Direction, Propeller + Duct fitted on

S. No.	V	n	$F_{T=0}$	t^*	T_S	P_d	P_e	η_d
	(m/s)	(rpm)	(N)			(W)	(W)	(%)
1	2.5	1089	81.4	0.0446	85.2	300.4	204.4	68.0
2	2.3	1004	66.9	0.0446	70.0	227.2	154.8	68.1
3	2.1	921	52.3	0.0439	54.8	172.6	110.4	63.9
4	1.8	832	38.0	0.0449	39.8	124.3	68.6	55.2
5	1.6	777	32.2	0.0468	33.7	100.0	51.7	51.6
6	1.3	694	22.3	0.0492	23.4	66.7	29.1	43.6
7	1.1	617	15.9	0.0507	16.8	44.0	17.6	39.9
8	0.8	500	7.7	0.0455	8.0	17.6	6.1	35.1

The " C-SCOUT " Vehicle (Figure 1)

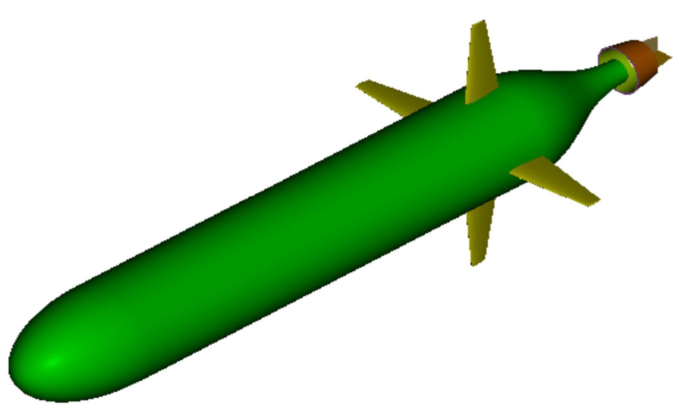

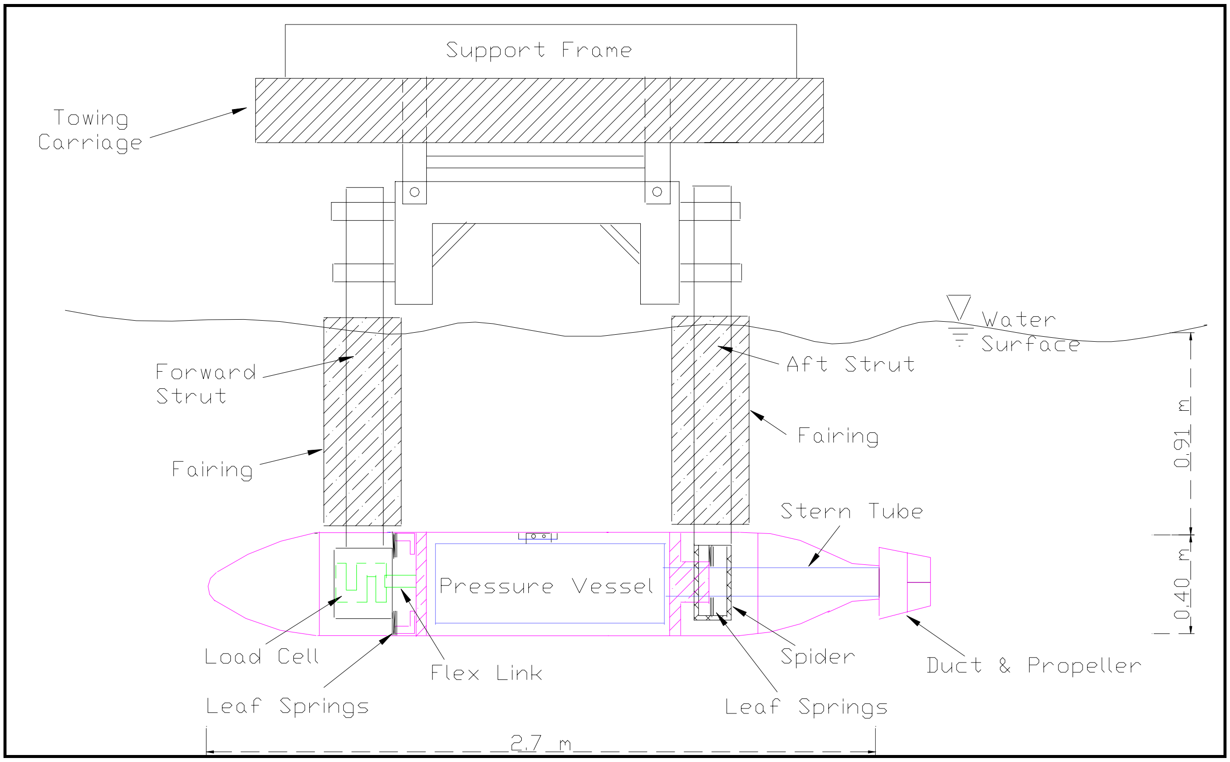

<u>Resistance & Propulsion Test Setup</u> (Figure 2)

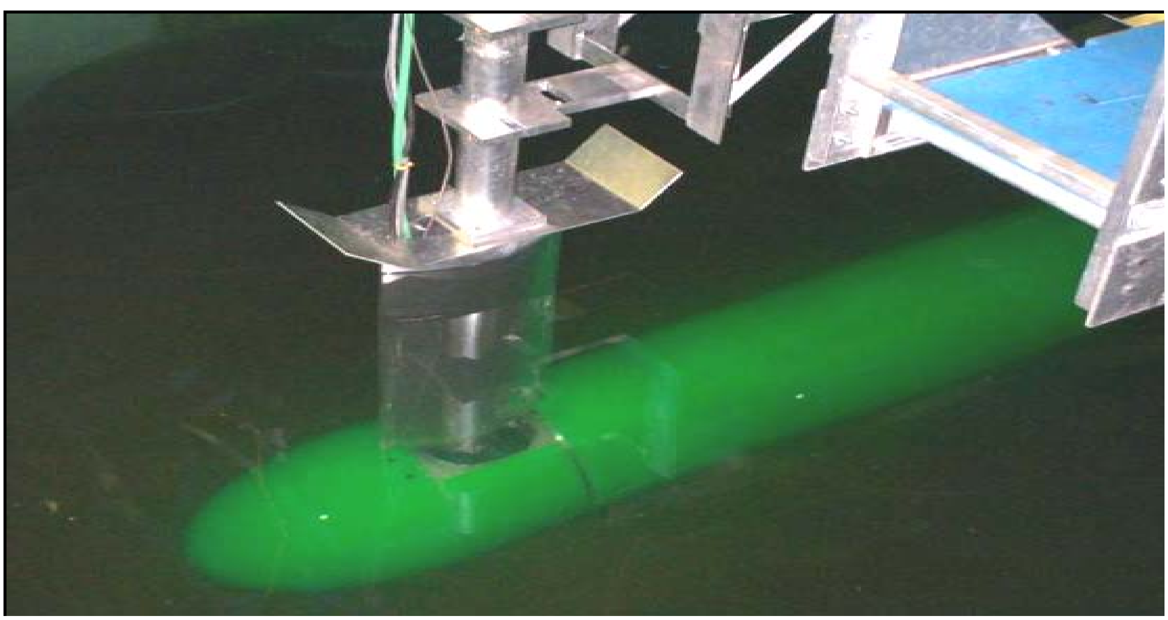

<u>Resistance & Propulsion Test Setup</u> (Figure 3)

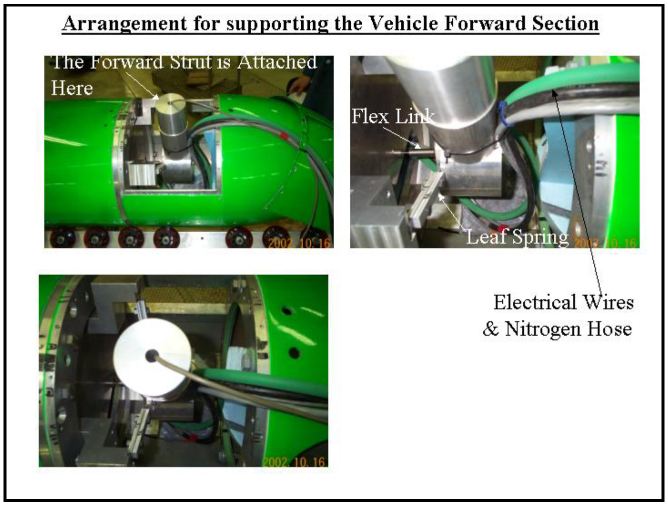

Forward Flexible Support (Figure 4)

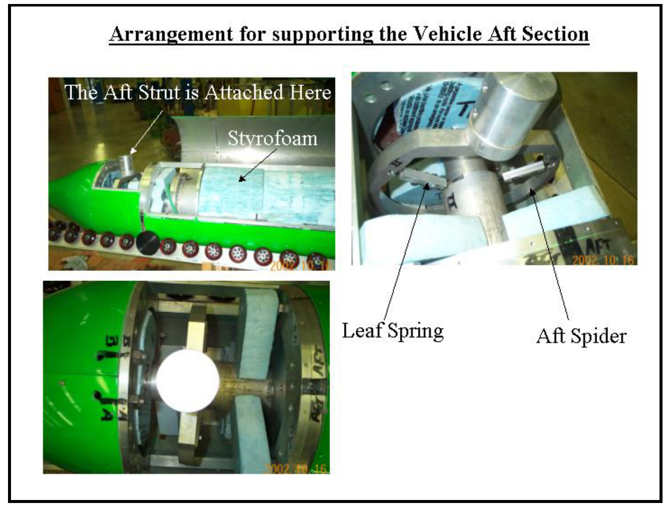

Aft Flexible Support (Figure 5)

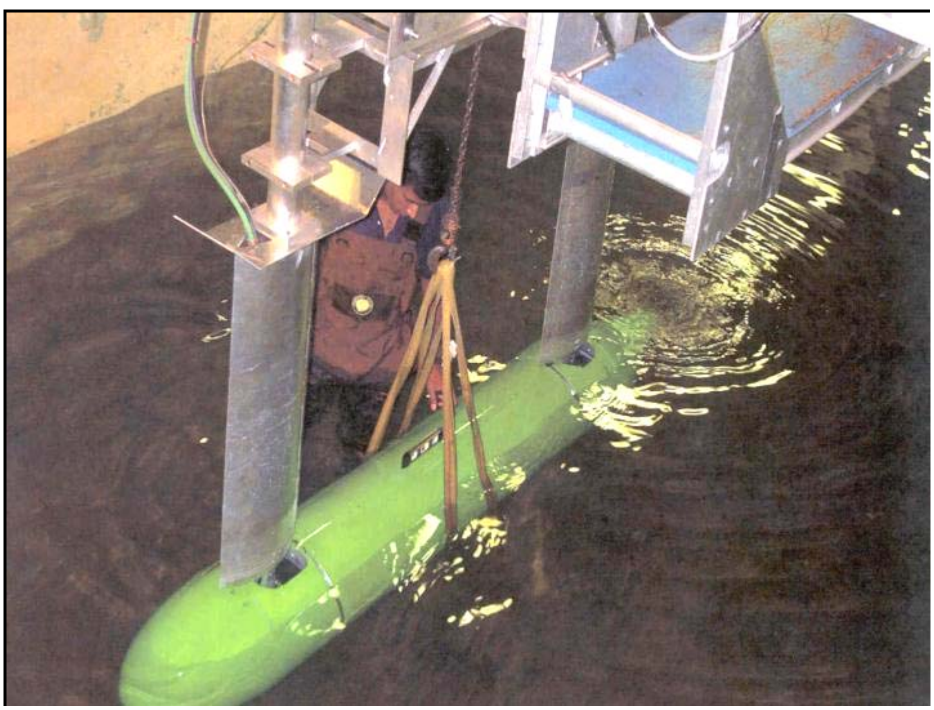

Vehicle Alignment Check (Figure 6)

Total Thrust vs Tow Force

(Load Varying Self - Propulsion Test, Ahead direction, Propeller + Duct fitted on)

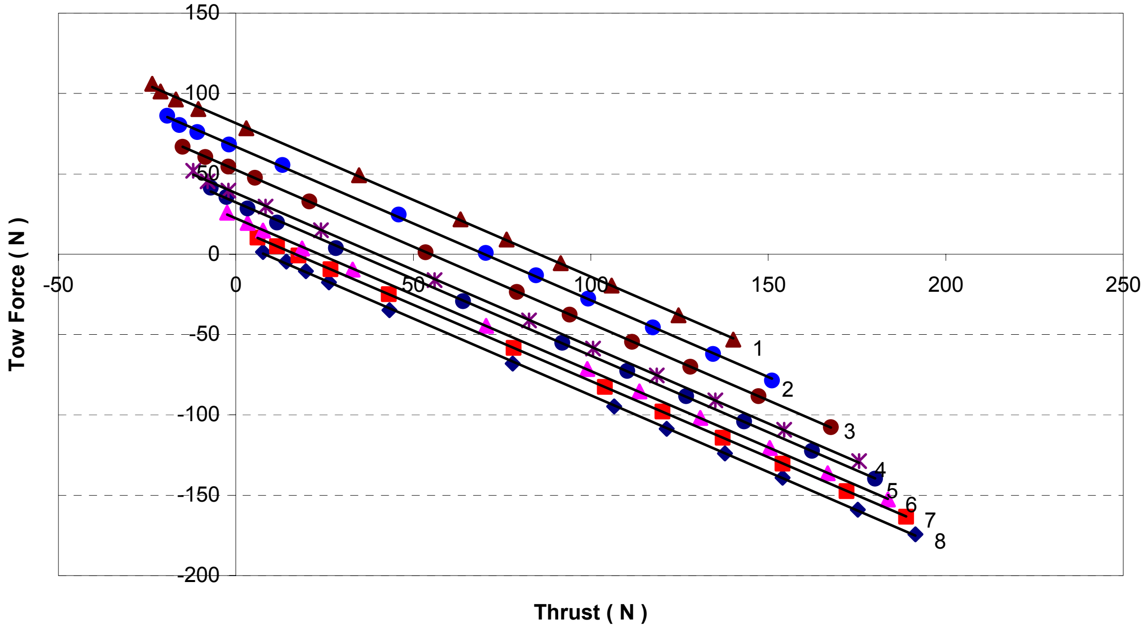

(Figure 7)

Load Varying Self - Propulsion Test

(V = 1.3 m / s , Ahead direction , only Propeller fitted on)

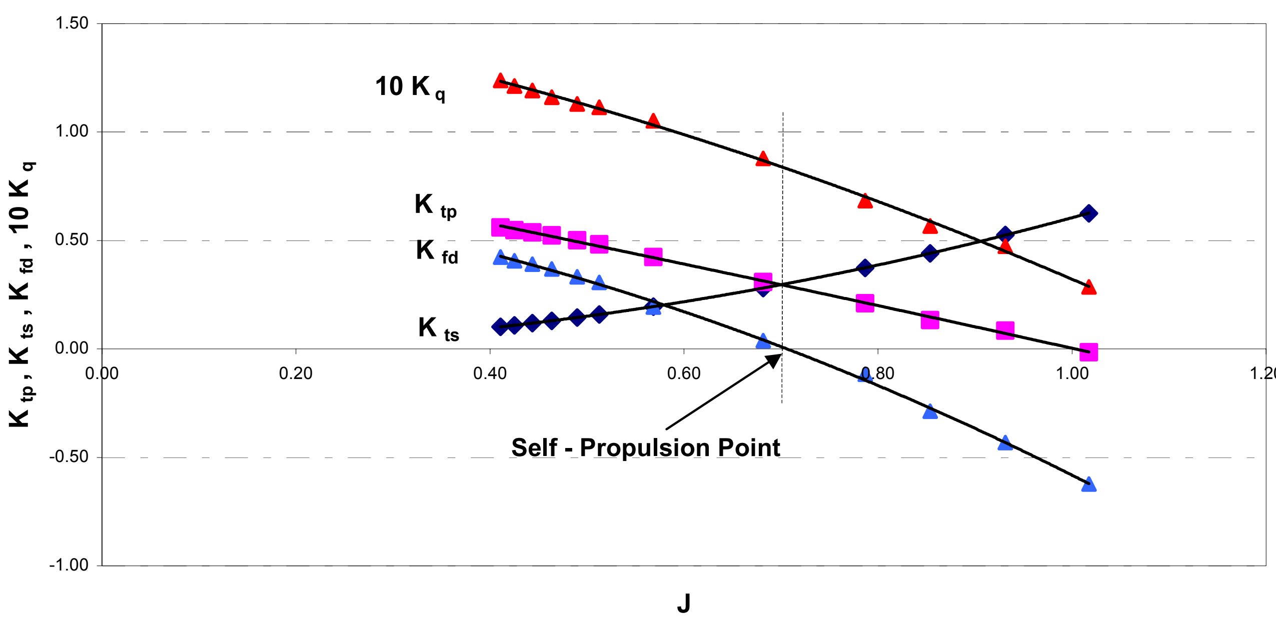

(Figure 8)

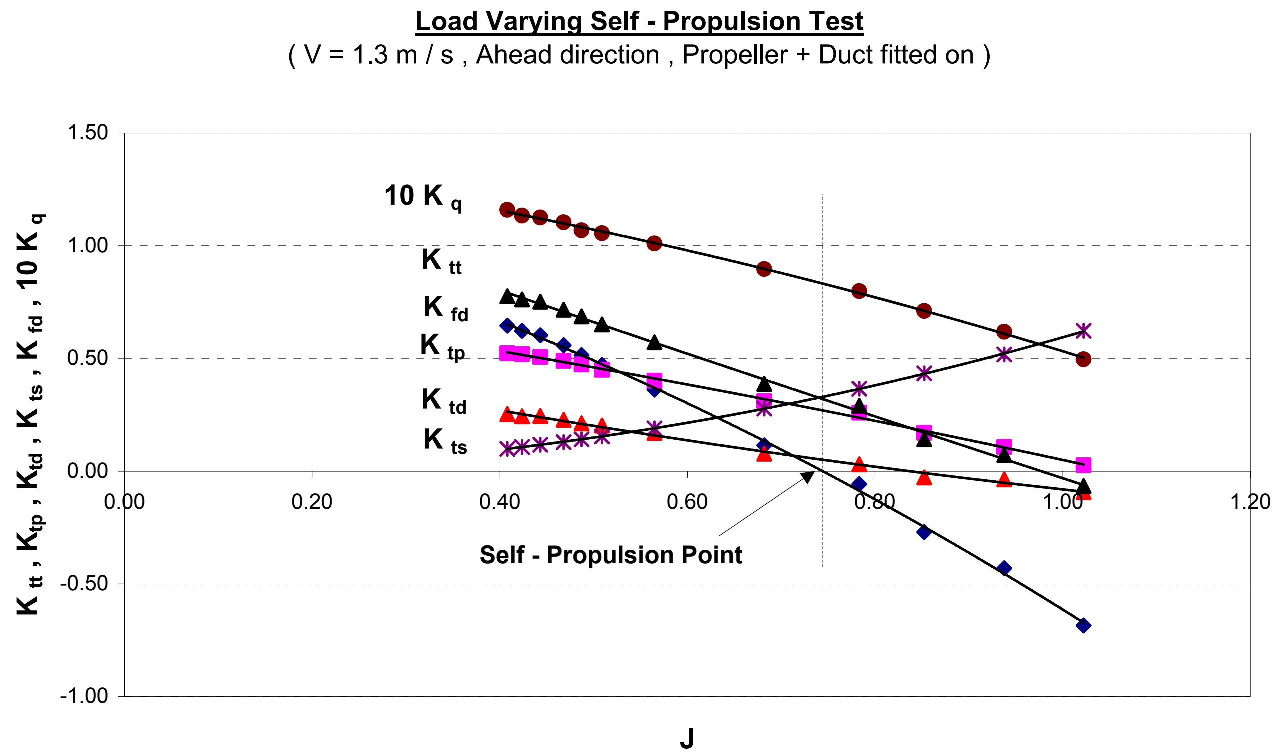

(Figure 9)

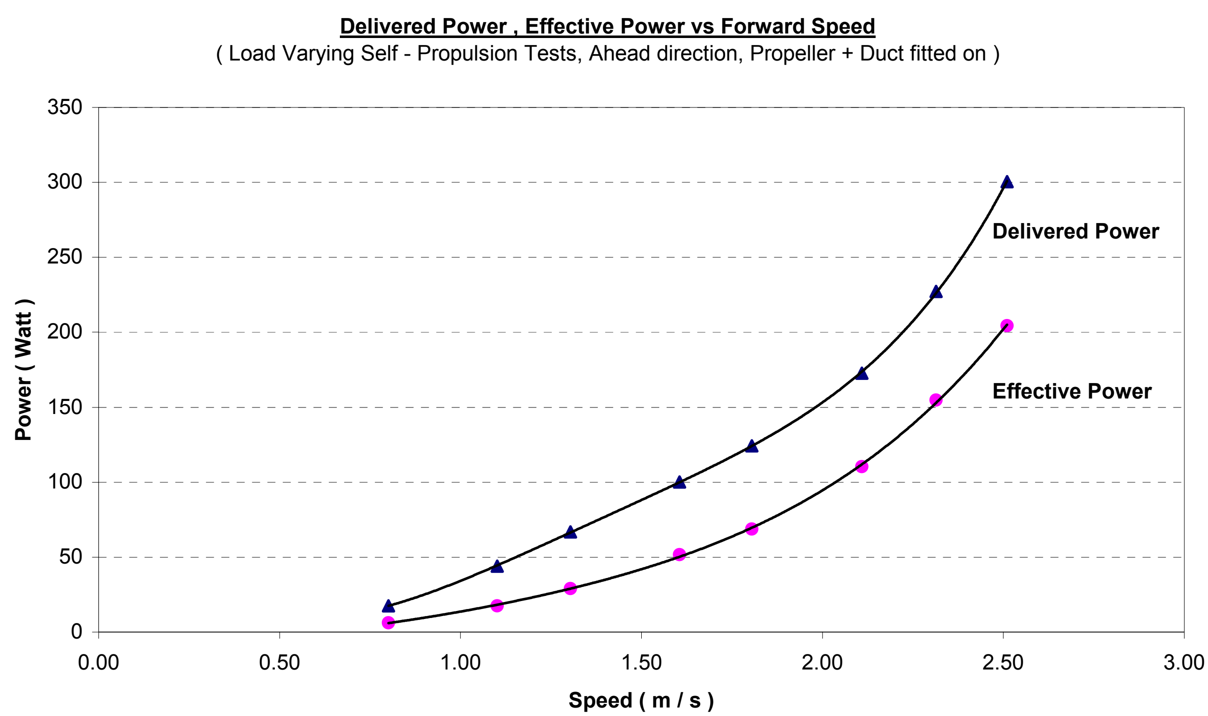

(Figure 10)

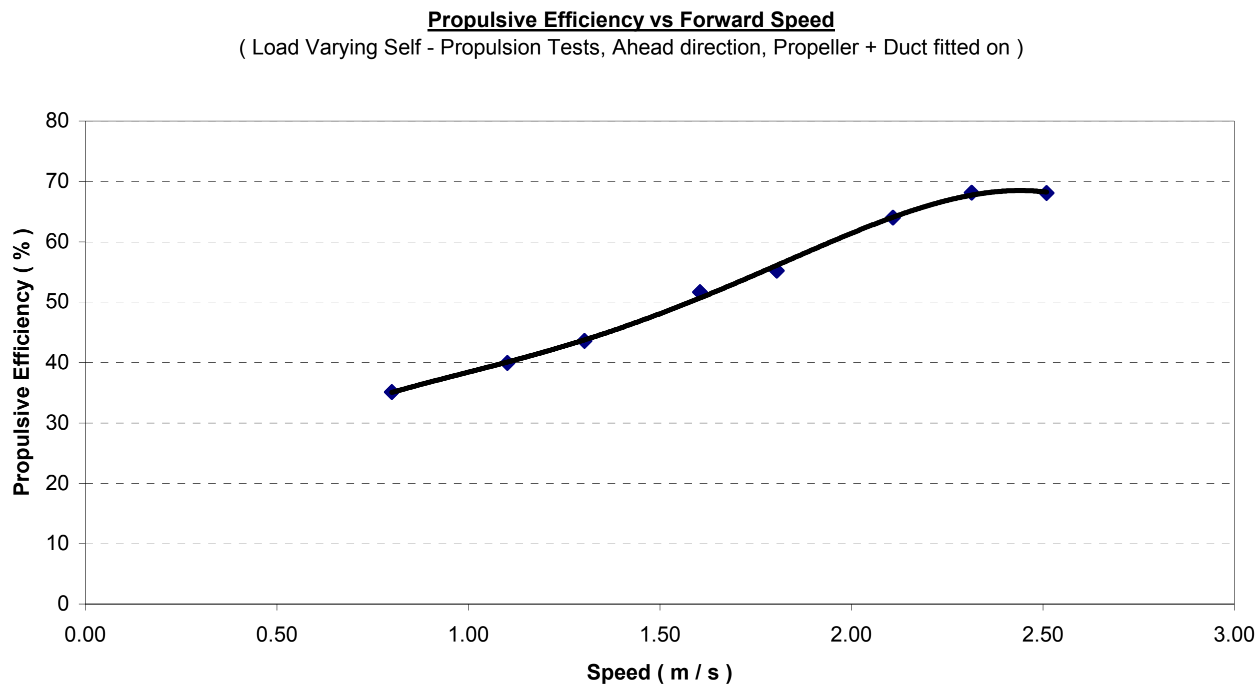

(Figure 11)

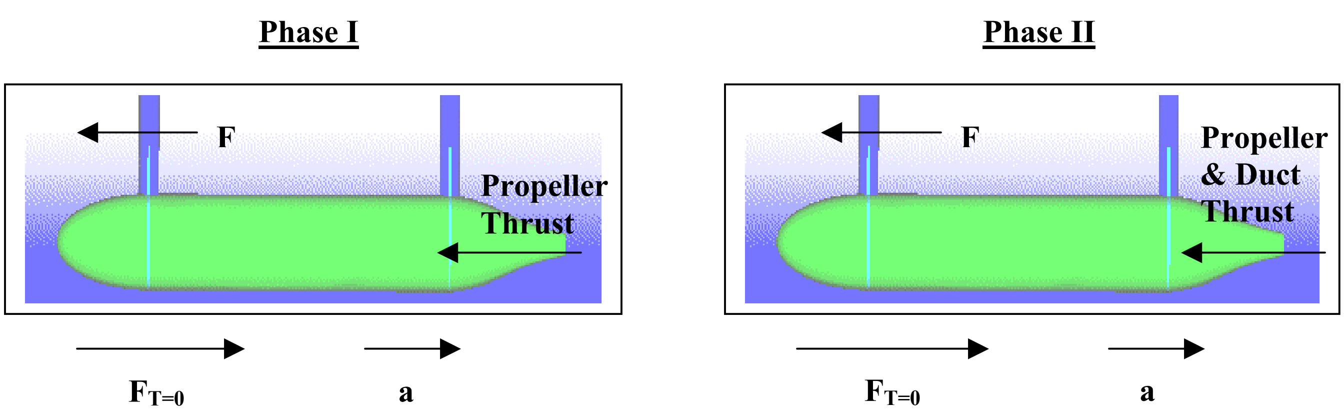

Forces acting on the Vehicle (Figure 12)

Bollard Pull Tests
(Tow Force , Thrust vs Propeller Speed)

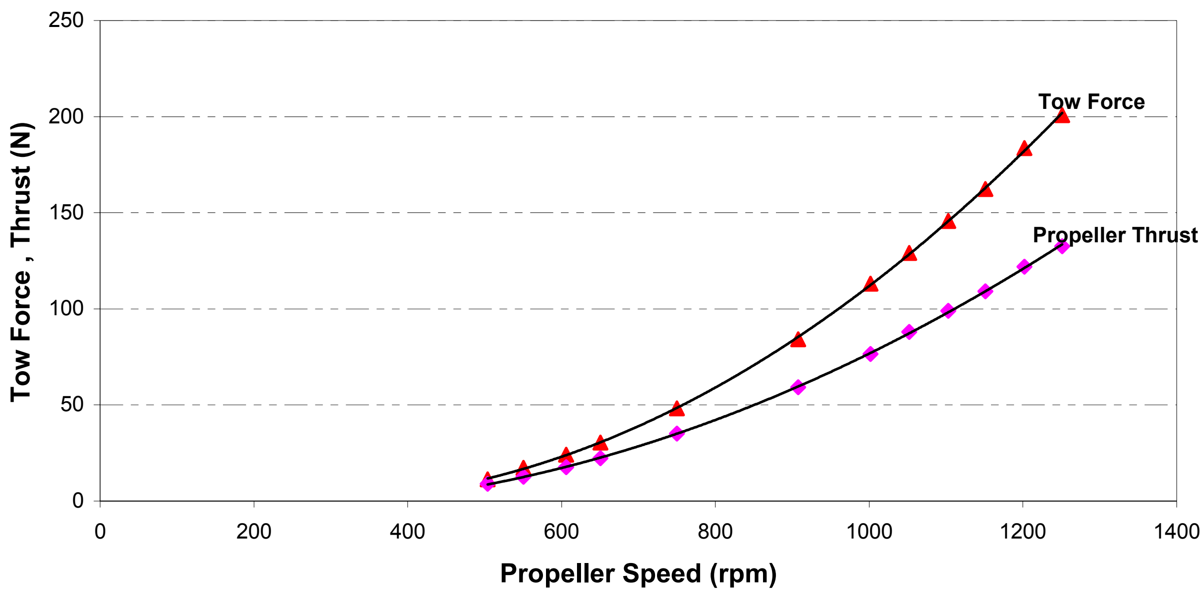

(Figure 13)

Bollard Pull Tests
(Delivered Power vs Propeller Speed)

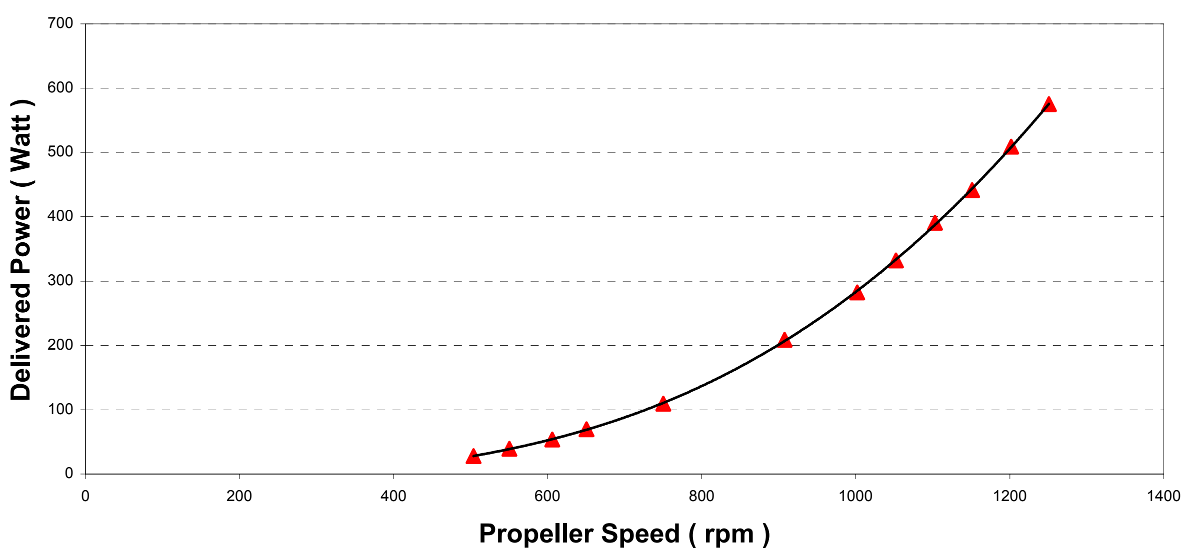

(Figure 14)

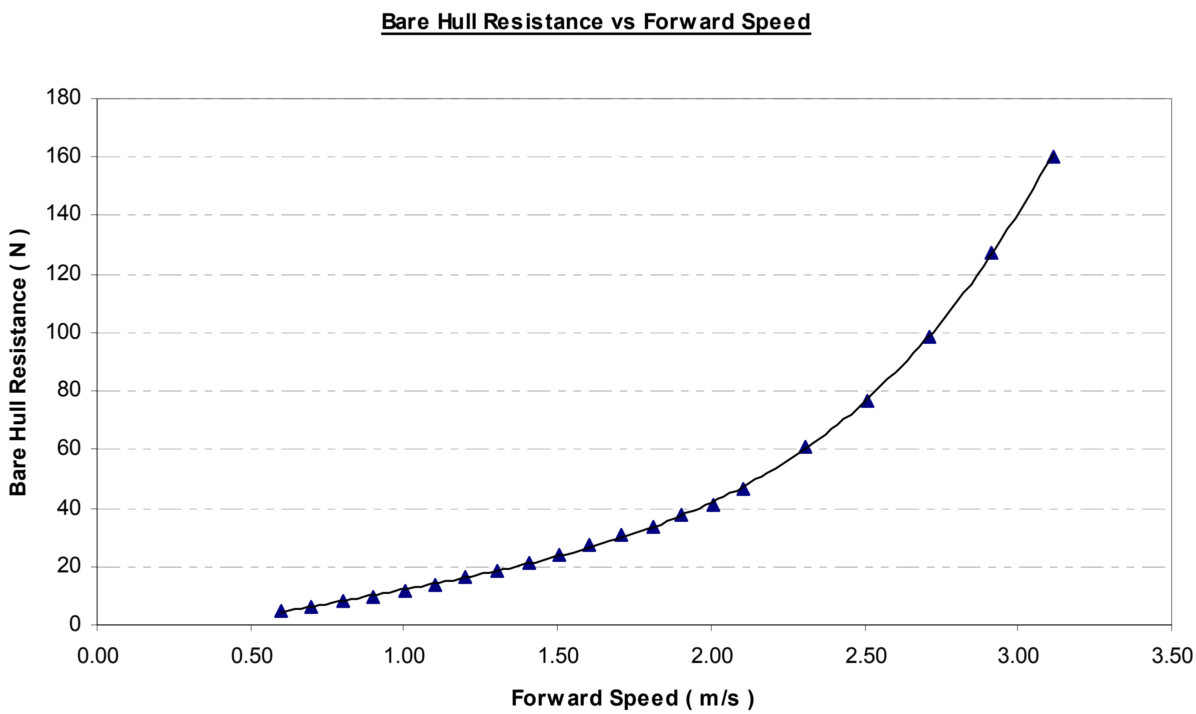

(Figure 15)

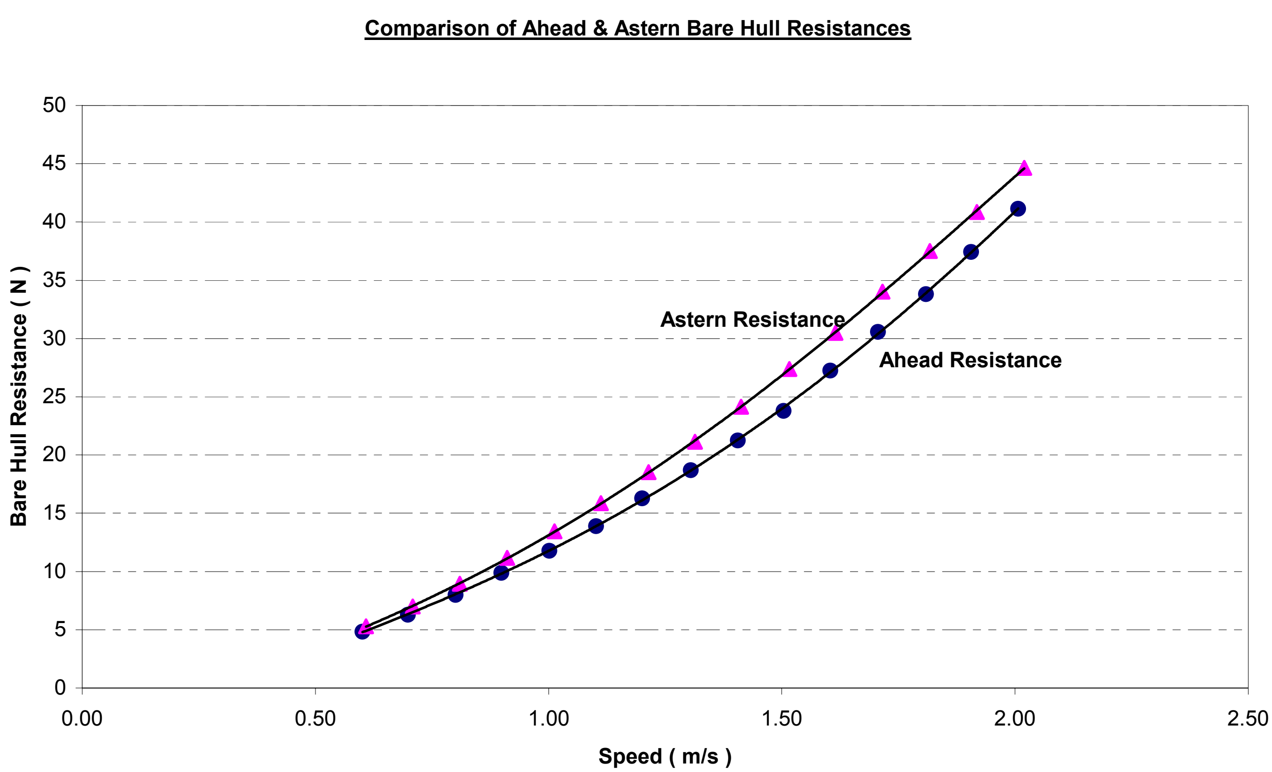

(Figure 16)

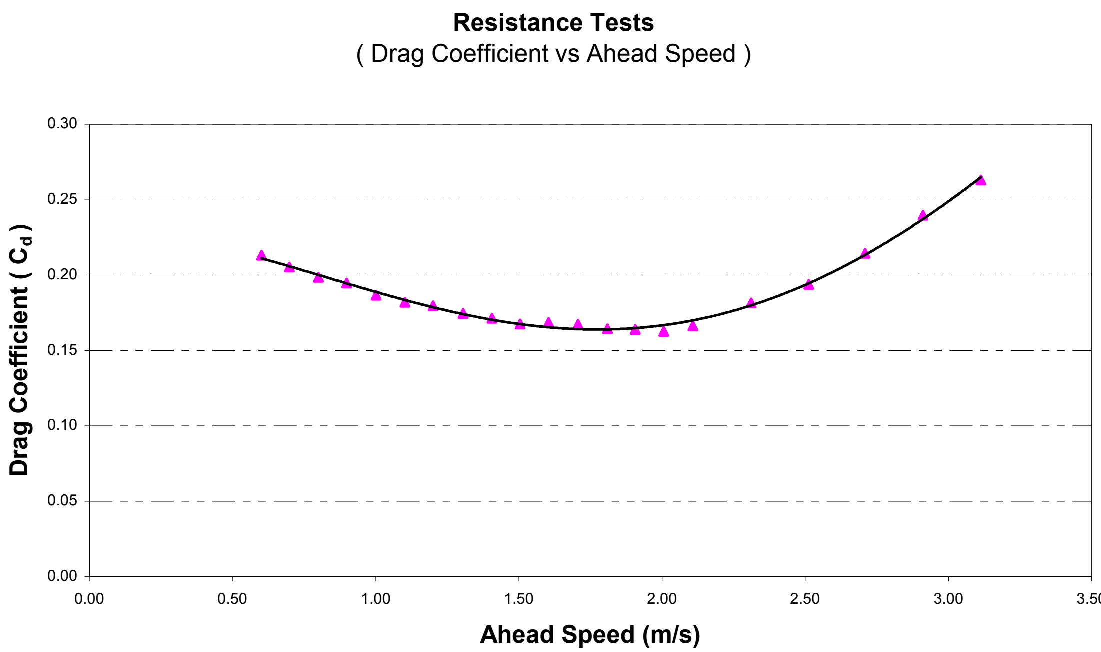

(Figure 17)

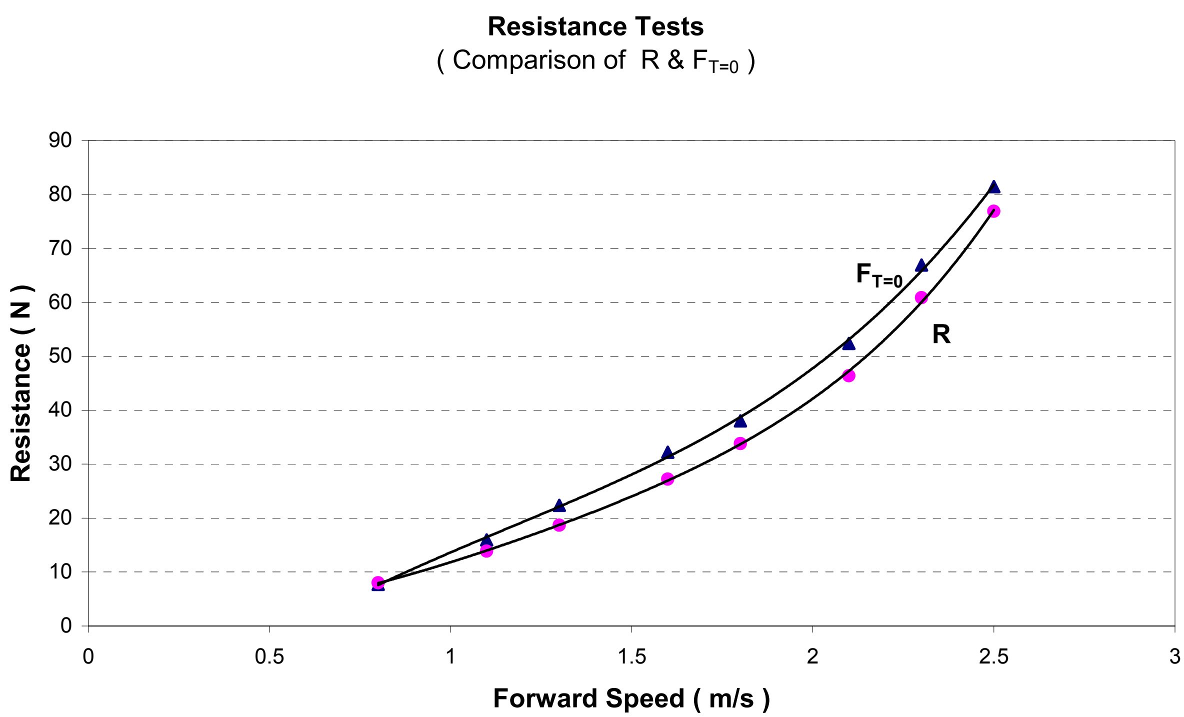

(Figure 18)